PNAS
www.pnas.org

# Supplementary Information for

Spontaneous seizure and memory loss in mice expressing an epileptic encephalopathy variant in the calmodulin-binding domain of Kv7.2

Eung Chang Kim[1], Jiaren Zhang[1], Andy Y. Tang[1], Eric C. Bolton[1], Justin S. Rhodes[2,3,4], Catherine A. Christian-Hinman[1,2,4], Hee Jung Chung[1,2,4*]

[1]Department of Molecular and Integrative Physiology, [2]Beckman Institute for Advanced Science and Technology, [3]Department of Psychology, [4]Neuroscience Program, University of Illinois at Urbana-Champaign, Urbana, IL 61801, USA.

***Corresponding Author:**
Hee Jung Chung
Department of Molecular and Integrative Physiology,
University of Illinois at Urbana-Champaign,
407 South Goodwin Avenue, 524 Burrill Hall,
Urbana, IL 61801, USA.
**Email:** chunghj@life.illinois.edu, chunghj@illinois.edu

**This PDF file includes:**

Supplementary text
Figures S1 to S14
Tables S1 to S4
Legends for Movies S1 to S5
SI References

**Other supplementary materials for this manuscript include the following:**

Movies S1 to S5

## Supplemental Methods

### 1. Experimental animals

All animal procedures were approved by the Institutional Animal Care and Use Committee of the University of Illinois at Urbana Champaign. Animals were housed in a controlled environment (12:12 h light/dark cycle with light on at 7 am and off at 7 pm, controlled humidity and temperature, free access to standard laboratory food and water) under the permanent supervision of professional technicians of the Division of Animal Research at the University of Illinois. At weaning, mice were group housed (up to 5 mice per cage) with littermates of the same sex.

### 2. Generation of transgenic *Kcnq2*-M547V$^{fl/fl}$ mouse line

The transgenic mice for conditional knock-in of mouse *KCNQ2* gene containing M547V mutation (ATG to GTG) (designated as *Kcnq2*-M547V$^{fl/+}$) on the C57BL/6J genetic background were generated at Cyagen Biosciences (Santa Clara, CA, USA) by well-established CRISPR/Cas-mediated genome engineering (1, 2). In *Kcnq2*-M547V$^{fl/+}$ mice, the transgene segment "CAG-LoxP-Stop-LoxP-*KCNQ2-M547V*-IRES-*EGFP*-polyA" were cloned into intron 1 of the Gt(ROSA)26Sor locus on mouse chromosome 6 (GenBank accession number: NR_027008.1) in a reverse direction. The donor vector was composed of a 2.5 kb homology arm and a 4.5 kb homology arm flanking the transgene, which consists of a CAG promoter and a floxed-STOP cassette upstream of mouse *KCNQ2 cDNA* containing M547V mutation (ATG to GTG) followed by an *IRES* sequence and *EGFP cDNA*. The homology arms were generated by Polymerase Chain Reaction (PCR) using BAC clone from the C57BL/6J library as template. The cassette and homology arms were fully sequenced and confirmed.

Cas9 and gRNA were co-injected into fertilized eggs with the donor vector for mice production. The gRNA used (GGCAGGCTTAAAGGCTAACCTGG) displayed a quality score indicative of great specificity and low off-target. The positive progenies were identified by genotyping with PCR and sequencing the PCR product. After this PCR selection step, Southern blotting was used to validate the 3' and 5' homology arm integration. After the implantation of the eggs into surrogate mothers, the resulting pups were screened by the PCR amplification and sequencing of the CRISPR-targeted site to identify the founders. The founders were confirmed by Southern Blot analysis and were bred to the C57BL/6J mice to obtain F1 mice at Cyagen Biosciences. We received 3 male and 3 female F1 *Kcnq2*-M547V$^{fl/+}$ mice from Cyagen Biosciences. In our lab, the *Kcnq2*-M547V$^{fl/+}$ line was backcrossed with C57BL/6J mice (Jackson Laboratory, Stock Number: 000664) for >5 generations and maintained on the C57BL/6J genetic background. These *Kcnq2*-M547V$^{fl/+}$ mice were crossed to each other to obtain homozygous *Kcnq2*-M547V$^{fl/fl}$ mice.

### 3. Induction of forebrain heterozygous expression of $K_v$7.2-M547V in *Kcnq2*$^{+/-}$ mice

To generate heterozygous knock-in of $K_v$7.2-M547V in mice, *Kcnq2*-M547V$^{fl/fl}$ mice were crossed to heterozygous *KCNQ2* gene knock-out (KO) mice (designated as *Kcnq2*$^{+/-}$) and Emx1-ires-cre (designated as Emx1$^{cre/cre}$). This strategy allows the expression of a single copy of *KCNQ2-M547V-IRES-EGFP* via cre-mediated removal of an upstream floxed-STOP cassette in heterozygous *KCNQ2* KO background. *Kcnq2*$^{+/-}$ mice and Emx1$^{cre/cre}$ mice (Stock Number: 005628) on the C57BL/6J background were obtained from the Jackson Laboratory. *Kcnq2*$^{+/-}$ mice contain a deletion in the mouse *KCNQ2* gene from base 418 to 535 on chromosome 2 (GenBank accession number: NM_010611.3) by insertion of a Lac0-SA-IRES-lacZNeo555G/Kan construct (*Kcnq2*$^{tm1Dgen/+}$, Jax.org Stock Number: 005830) (3). Emx1$^{cre/cre}$ mice express Cre recombinase in neocortical and hippocampal pyramidal neurons during neurogenesis starting at embryonic (E) day 10.5 (Jax.org Stock Number: 005628).

The resulting progenies are *Kcnq2*-M547V$^{fl/+}$: *Kcnq2*$^{+/-}$: Emx1$^{cre}$/$^{+}$ mice (designated as *cKcnq2*$^{+/M547V}$ mice), *Kcnq2*-M547V$^{fl/+}$: Emx1$^{cre}$/$^{+}$ mice (designated as *cKcnq2*$^{pyr-M547V}$ mice), *Kcnq2*$^{+/-}$ mice, and wild type control mice (*Kcnq2*- M547V$^{fl/+}$, Emx1$^{cre}$/$^{+}$ mice, *Kcnq2*$^{+/+}$). The

*cKcnq2*$^{+/M547V}$ mice express a single copy of *KCNQ2-M547V-IRES-EGFP* in forebrain excitatory pyramidal neurons in *Kcnq2*$^{+/-}$ mice, whereas *cKcnq2* $^{pyr-M547V}$ mice express a single copy of *KCNQ2-M547V-IRES-EGFP* in forebrain excitatory pyramidal neurons in *Kcnq2*$^{+/+}$ mice. The control mice used in these studies were *Kcnq2*$^{+/+}$, *Kcnq2*- M547V$^{fl/+}$, *Kcnq2*- M547V$^{fl/fl}$, Emx1$^{cre}$/$^{+}$, Emx1$^{cre}$/$^{cre}$ mice.

**4. Genotyping**

Genotyping was determined by PCR on the genomic DNA prepared from mouse tails. The primers used in genotyping *Kcnq2*-M547V$^{fl/+}$ mice were the forward primer specific for the cassette "CAG-LoxP-Stop-LoxP-*KCNQ2-M547V*-IRES-*EGFP*-polyA" (5'- CAC TTG ATG TAC TGC CAA GTG G-3'), as well as the forward primer (5'-CAC TTG CTC TCC CAA AGT CGC TC-3') and the reverse primer (5'- ATA CTC CGA GGC GGA TCA CAA -3') that anneal to the 5' and 3' end of intron 1 of endogenous ROSA26 gene, respectively. Genotyping of Emx1$^{cre/+}$ and Emx1$^{cre/cre}$ mice was determined by PCR using primers to *cre* including the forward primer (5'- CGA CCA GGT TCG TTC ACT CA-3') and the reverse primer (5'- CGA GTT GAT AGC TGG CTG GT-3'). Genotyping of *Kcnq2*$^{+/-}$ mice was determined by PCR as described (4) using primers against endogenous *Kcnq2* gene and the truncated *Kcnq2* gene (target gene) which is present only in *Kcnq2*$^{+/-}$ mice (3). The primers used were the forward primer common to both target and endogenous genes (5'-ATC GTG ACT ATC GTG GTA TTC GGT G-3'), the reverse primer to endogenous genes (5'-GGT GAT AAG AAG GAA CTT CCA GAA G-3') and the Neo reverse primer specific for the target gene only (5'-GGG CCA GCT CAT TCC TCC CAC TCA T-3').

**5. Video-EEG monitoring in freely moving mice**

To examine spontaneous seizures, mice were subjected to a video electroencephalogram (EEG) monitoring system (Pinnacle Technology) as described (5, 6). The surgical implantation of electrocorticographic electrodes was performed on mice at P53-77 under sterile conditions. Mice were deeply anesthetized with 4% isoflurane in 100% oxygen and received subcutaneous (s.c.) injection of carprofen (5 mg/kg). Isoflurane was delivered through an anesthesia mask and was gradually decreased from 4% to 1.5 %. Mice were placed in the stereotaxic apparatus (Kopf Instruments) above a heating pad to maintain body temperature at 36°C throughout the surgical procedure. An ophthalmic gel (Systane gel, Alcon, USA) was placed on eyes to prevent dryness. The shaved scalp was cleaned with betadine and 70 % ethanol. After the scalp was removed, the bone surface was cleaned. Four insulated silver wire electrodes (Cat No. 76000, A-M Systems) connected to an 8-pin surface mouse headmount (Cat No. 8415-SM, Pinnacle Technology) were placed so that 2 subdural cortical electrodes were inserted bilaterally in the frontal areas and the 2 others in the parietal areas. Electrodes and mouse headmount were secured at the surface of the skull using Vetbond (3M), and the implant was secured to the skull using dental cement. After surgery, the mouse received a s.c. injection of 0.5 ml saline and treated with anesthetic cream (lidocaine and prilocaine) and Neosporin ointment on the skin around the base of dental cement.

After 1 week of recovery, mice were individually placed into a Plexiglas cylinder (Pinnacle Technology) and its microconnectors plugged to an EEG preamplifier (Pinnacle Technology). EEG and simultaneous video were recorded from 2-4:30 PM relative to lights-off time of 7 PM. The electrical signal was band pass filtered at 1–100 Hz, digitized at 200 Hz, and acquired with a computer-based system (Pinnacle Technology). EEG spikes were clearly distinguishable from baseline EEG activity by their repetitive occurrence, large amplitude (> 2-fold background), and sharp morphology (5, 7). The peaks in the baseline activity and the electrographic activity were measured after setting the threshold of 25 μV and 75 μV, respectively. Spontaneous seizures were visually confirmed by analyzing behavioral seizures in the video recordings.

**6. Kainic acid-induced seizures**

To measure seizure susceptibility in response to kainic acid, mice were subjected to intraperitoneal (i.p.) injection of vehicle control (saline) or kainic acid (KA) (15 mg/kg, Abcam) as described (4).

The mice were at 4- to 6-month old (P120-P180) when KA injections were performed. Mice were returned to their home cage and monitored for behavioral seizures every 10 minutes (min) for 2 hours (h) using a modified Racine, Pinal and Rovner scale (8).

**7. Mice for behavioral studies**

A total of 19 male mice (control n=8; *cKcnq2*$^{+/M547V}$ n=11) and a total of 19 female mice (control n=8; *cKcnq2*$^{+/M547V}$ n=11) were used for behavior tests in a separate behavioral test room under a "reverse" light:dark schedule with lights off at 10 am and lights on at 10 pm. Before the first behavioral test, all test mice and novel social target mice were habituated to "reverse" light:dark cycle and handled twice daily for 2 weeks. All mice were weighed and subjected to a battery of behavior tests in the following order: object location and novel object recognition tasks, self-grooming, marble burying, open field, rotarod, and social interaction tests. This order allows the tests to be conducted from the least invasive to most invasive tests. Each test was performed at least 2 days after the previous test to minimize the potential impact of one behavioral assay to the subsequent ones (9, 10).

**7.1 Novel object recognition test and object location test**

The novel object recognition task (NORT) and object location task (OLT) were performed to examine the memory of mice for previously encountered objects as described (11). The test was conducted in the Opaque White Acrylic square box (40 × 40 × 40 cm) containing environmental visual cues on each wall. The test was performed in 4 phases: habituation, training, OLT, and NORT. During habituation, each mouse was allowed to explore the field in the absence of objects for 6 min 3 times with the inter-trial interval (ITI) of 10 min to make them familiar with the field. During the training trial on next day, two objects were placed symmetrically onto the arena. A mouse was placed facing the walls of the release corner in the area that has no object, and was allowed to freely explore for 10 min. The mouse was returned to its home cage for ITI of 20 min. The mouse was then subjected to the OLT test, in which one of the two objects used in the training trial was moved to a new non-release corner, and the mouse was allowed to investigate the objects for 10 min. After an ITI of 20 min, mice were subjected to the NORT test, in which a novel object replaced the object which was not moved during the OLT. The mouse was re-introduced to the release corner and allowed to explore for 10 min. The arenas and objects were cleaned with 70% ethanol to minimize olfactory cues during each ITI. The TopScan video tracking system and software (CleverSystems, Reston, VA, USA) were used to collect behavioral performances automatically. The time spent exploring both novel and familiar objects was recorded. A mouse was scored as exploring an object when its head was oriented toward the object and within a distance of 1 cm, or when its nose was touching the object. Discrimination Index (DI) was calculated as ($Time_{novel} - Time_{familiar}$)/($Time_{novel} + Time_{familiar}$).

**7.2 Self-grooming**

Self-grooming behavior of the mice was examined to assess their repetitive behaviors as described (12). The test mouse was placed in its home cage without bedding and video monitored for 10 min. The duration and latency of each grooming event and the total number of grooming events of each mouse was quantified.

**7.3 Marble burying test**

Marble burying test was performed to monitor repetitive and compulsive-like behaviors in mice as described (13). A novel cage was half filled with fresh 5 cm-deep bedding. Twenty marbles were placed on top of the bedding and arranged in a 4 by 5 array. The mouse was placed in this cage and allowed to spontaneously bury marbles for 30 min. After removing the mouse, the cage floor was photographed. A marble that was more than two-thirds under bedding was considered "buried" and counted. Each mouse was tested in a new cage with fresh bedding and marbles.

### 7.4 Open field test

The open field test was used to assess anxiety and exploratory behavior in mice as described (14). The test was conducted in an open field arena (26 in. × 26 in. × 12 in.). The mouse was placed in the center of an arena and allowed to explore for 5 min. The mouse behavior was recorded by TopScan video-tracking system to compute the distance traveled throughout the arena as well as the number of entries into and duration in the central square (14 in. × 14 in., 6 in. away from the sides). The arena was cleaned between each mouse.

### 7.5 Rotarod test

Rotarod testing was performed to assess motor coordination as described (15). Mice were placed on the rotarod apparatus and then the start switch was turned on to rotate the dowel a constant acceleration rate of 60 rotation per min (rpm). The latency of the mice to fall off the apparatus was recorded by photobeam counters and an experimenter using a stopwatch. The average latency from 3 trials was computed per mouse. The dowel was cleaned between each trial.

### 7.6. Three-chamber social interaction test

The three-chamber social interaction test was performed to examine sociability as described (16). The test was conducted in the clear Plexiglas three-chamber rectangular arena in which each chamber (20 × 40 × 25 cm) has rectangular openings (5 × 8 cm) for the mouse to access 3 chambers. The test was performed in 3 sessions of 10 min: habituation, sociability and social novelty. The chambers were thoroughly cleaned between sessions after removing the mouse from the arena. During habituation, the test mouse was placed in the center chamber and allowed to freely explore the empty chambers without empty cylinder wire cages (15 cm diameter and 20 cm height) for 10 min and then with cages for additional 10 min. During habitation, all tested mice displayed no preference for either a left or a right chamber. In the “sociability” session, a C57BL/6J mouse of the same sex (a stranger mouse-1) was placed underneath the wire cage in the right chamber. The test mouse was then placed in the center chamber and allowed to freely explore for 10 min. In the “social novelty” session, another C57BL/6J mouse of the same sex (stranger mouse-2) was placed underneath the wire cage in the left chamber. The test mouse was then re-introduced in the center chamber and allowed to freely explore for 10 min. The TopScan video tracking system automatically recorded the mouse sniffing behavior, which is defined by the physical contacts between the boundaries of the object and the mouse nose, head and forelimbs (17).

### 8. Mouse hippocampi fractionation

After carbon dioxide ($CO_2$) euthanasia of the mice, their brains were dissected for specific brain regions (hippocampi, cortexes, and cerebellums) and stored in -80°C. The dissected forebrain per mouse (for P1) or hippocampi per mouse (for P30, P60, P120) were homogenized in ice-cold homogenization buffer (solution A) containing (in mM): 320 sucrose, 1 $NaHCO_3$, 1 $MgCl_2$, 0.5 $CaCl_2$, 0.4 HEPES (pH 7.4) and Halt protease inhibitors (Thermo Fisher Scientific) as described (18). The homogenate was centrifuged 1400 x g for 10 min at 4°C to separate the homogenate supernatant (S1) from insoluble tissue and nuclear pellet (P1). The S1 fraction was then centrifuged at 13,800 x g for 10 min at 4°C to separate the supernatant (S2 soluble fraction enriched with cytosolic soluble proteins) from the pellet (P2 membrane fraction enriched with transmembrane proteins and membrane-bound proteins). The pellet (P2) was resuspended in ice-cold solution B containing (in mM): 160 sucrose, 6 Tris-HCl, 0.5% Triton-X (pH 8.0) and Halt protease inhibitors. Protein concentrations of the S1, S2, and P2 fractions were determined by BCA assay (Pierce). The S1, S2, and P2 fractions were normalized to 0.5 mg/ml in Solution A (pH 7.4), and stored at -80°C until use.

### 9. CHOhm1 cells transfection and lysate preparation

CHOhm1 cells were plated on 35 mm tissue culture dishes (Corning, 3 x $10^5$ cells per well). Next day, cells were transfected with pcDNA3-$K_v$7.2 WT or mutant (0.5 μg) using FuGENE6 transfection reagent (Promega). At 24 hours post transfection, cells were lysed, and lysates were analyzed by immunoblotting as previously described (19). Briefly, cells were collected by cell scraper in 300 μL ice-cold lysis buffer containing (mM): 150 NaCl, 50 Tris, 2 EGTA, 1 EDTA, 1% Triton-X, 0.5% deoxycholic acid, 0.1% SDS (pH 7.4), supplemented with Halt protease inhibitor cocktail (Thermo Fisher Scientific). After 15 min incubation on ice, the cells in lysis buffer were centrifuged at 14,000 x g for 15 min in 4 °C. The supernatant (lysate) was transferred to clean tubes and subjected to SDS-PAGE electrophoresis.

**10. SDS-PAGE electrophoresis and immunoblotting**

Samples (hippocampal P2 fraction, or CHOhm1 cell lysate) were mixed with SDS sample buffer in 1:5 ratio and heated at 75 °C for 30 min. The SDS sample buffer contained (mM): 75 Tris, 50 TCEP, 0.5 EDTA, 10% SDS, 12.5% glycerol, 0.5 mg/mL Bromophenol Blue. The samples were then run on 4%-20% gradient SDS-PAGE gels (Bio-Rad) and transferred to a methanol-treated polyvinyl difluoride (PVDF) membrane (Millipore). The membranes were blocked with blocking buffer (5% nonfat milk/0.1% Tween-20 in Tris-buffered saline/TBS containing 150 mM NaCl, 50 mM Tris, pH 7.5) for 1 h followed by overnight incubation of primary antibodies in washing buffer (1% nonfat milk/0.1% Tween-20 in TBS) in 4 °C. After 1 h incubation with horse radish peroxidase-conjugated secondary antibodies in washing buffer, membranes were treated with Enhanced Chemiluminescence substrate (ECL, Thermo Fisher Scientific) and immediately developed with a Konica SRX-101A film processor (for hippocampal P2 fraction) or imaged with the iBright CL1000 imaging system (for CHOhm1 cell lysate). Acquired images were analyzed using ImageJ software (National Institute of Health). GAPDH and β-tubulin were used as loading controls. Background-subtracted intensities of each immunoblot band was measured and the $K_v$7.2/loading control ratio of WT or mutants was computed. The $K_v$7.2/loading control of WT was used as 100% and mutants were normalized to WT as described (19). Antibodies used for immunoblotting hippocampal P2 fraction include anti-$K_v$7.2 (Synaptic Systems, #368103, 1:1000 dilution) and anti- β-tubulin (Cell Signaling #2144, 1:500 dilution). Antibodies used for immunoblotting transfected CHOhm1 cell lysate include anti-$K_v$7.2 (Synaptic Systems, #368103, 1:1000 dilution) and anti-GAPDH (Cell Signaling #2118, 1:1000 dilution), donkey anti-rabbit and donkey anti-mouse HRP secondary antibodies (The Jackson Laboratory, 711-035-152; 715-035-150, 1:2500 dilution).

**11. CHOhm1 cells transfection and immunostaining**

CHOhm1 cells were plated on 12 mm glass coverslips (Warner Instrument, 5 x $10^4$ per coverslip) pretreated with poly D-lysine (0.1 mg/mL) (Sigma-Aldrich). Next day, the cells were transfected with pEGFPC1 and pcDNA3 (empty vector control), pcDNA3-$K_v$7.2, pcDNA3-$K_v$7.2-M518V using FuGENE6 transfection reagent (Promega). Plasmid pcDNA3 carrying *KCNQ2* cDNA (GenBank: Y15065.1) encoding a short isoform of human $K_v$7.2 (GenBank: CAA 75348.1) was previously described (19-21). This short isoform of $K_v$7.2 lacks 2 exons compared to the reference $K_v$7.2 sequence (GenBank: NP_742105.1). At 24 h post transfection, immunostaining was performed as described (19). In brief, the coverslips were washed once with PBS, fixed in 4% (w/v) paraformaldehyde and 4% sucrose in PBS for 20 min, and permeabilized with 0.2% Triton X-100 in PBS for 30 min. The coverslips were incubated in 10% normal donkey serum (NDS) (Jackson ImmunoResearch) for 1 h at room temperature, and treated with rabbit anti-$K_v$7.2 antibody (Synaptic Systems, #368103, 1:500 dilution) in 3% NDS in PBS at 4°C overnight. The coverslips were washed with PBS and incubated with donkey anti-rabbit Alexa594-conjugated secondary antibody (Thermo Fisher Scientific, A21207, 1:300 dilution) for 2 h at room temperature. The coverslips were washed in PBS and mounted using Fluorogel anti-fade mounting medium (Electron Microscopy Sciences). Grey-scale images were taken using a Zeiss Axio Observer inverted microscope with a 20X objective, a ZeissCam 702 mono Camera, and Zen Blue 2.6 software.

**12. Immunocytochemistry of mouse brain cryosections**

Mice were deeply anesthetized with a mixture of ketamine hydrochloride (100 mg/kg, Dechra) and xylazine hydrochloride (10 mg/kg, Bimeda)(s.c. injection). They were subjected to a transcardial perfusion via the left ventricle with 30 mL chilled PBS solution containing heparin (100 unit/ml) followed by 30 mL 2% (wt/vol) paraformaldehyde (PFA, Sigma Aldrich, pH 6.0 with acetic acid) in PBS. Brains were post-fixed in the same fixative for 24 h at 4°C, cryoprotected for 24 h in 30% (wt/vol) sucrose in PBS at 4°C, and stored in anti-freeze O.C.T. compound (Fisher Scientific) at −70 °C. Coronal brain sections (20 µm thick) were prepared using a cryostat microtome (Leica CM 3050S; Leica Microsystems) and mounted on Superfrost Plus slides (Thermo Fisher Scientific). Cryosections was post-fixed for 30 min with 4% paraformaldehyde in PBS (pH 7.4), washed with PBS, permeabilized 0.3% Triton X-100 (Alfa Aesar) in PBS for 30 min, and blocked with 10% normal goat serum (NGS, Jackson ImmunoResearch) in PBS for 30 min. The slices were incubated with primary antibodies in 3% NGS in PBS overnight at 4°C. To immunostaining $K_v7.2$ and Ankyrin-G (AIS marker), the post-fixation omitted, and the sections were blocked in 0.5% Triton X-100 and 5% NGS in PBS for 30 min, and incubated with the primary antibodies in the same blocking buffer. The following antibodies were used: mouse anti-GFAP (1:200, Neuromab), rabbit anti-NeuN (1:500, Cell signaling), rabbit anti-$K_v7.2$ (1:500, Synaptic system), mouse anti-Ankyrin-G (1:500, Neuromab), and chicken anti-GFP (1:500, Abcam, due to weak endogenous GFP fluorescence in *cKcnq2*$^{+/M547V}$ mice). Sections were rinsed with PBS solution and incubated with secondary antibodies overnight at 4°C. The following secondary antibodies (all from Thermo Fisher Scientific) were used: goat anti-mouse Alexa 680 (1:500), goat anti-rabbit Alexa 594 (1:500), and goat anti-chicken Alexa 488 (1:1500). Sections were rinsed with PBS, counterstained with DAPI (1:200, Thermo Fisher Scientific), and mounted with Vectashield antifade mounting medium (Vector Laboratories).

Fluorescent images (160.04 µm x 160.04 µm with a 40X objective; 101.61 µm x 101.61 µm with a 63X objective) with an optical distance of 1 µm were obtained using a laser scanning Zeiss LSM 700 confocal microscope. The laser power and photomultiplier gain were set at the same levels for all sections. The pyramidal cell and dendritic layers of CA1, CA3, and the dentate gyrus (DG) of hippocampus at a single section were selected for analysis using ImageJ software (NIH). To count the numbers of GFAP-positive astrocytes and measure mean fluorescence intensity of GFAP, background intensities were first determined within each image through the sampling of four independent regions of interest (ROI) containing no astrocytes in ImageJ. The mean fluorescence intensities of the four chosen non-astrocyte regions were averaged to give an overall background intensity for each image. Next, an image quantification algorithm titled “ANIMA” (described in a later section 12) was used to automatically identify and quantify mean fluorescence intensity of astrocytes which fully engulf one or more nuclei in each image. Each image was subsequently manually reviewed to ensure all selected astrocytes indeed meet the criteria for selection.

**13. Development of the ANIMA Image Quantification Algorithm**

An algorithm for image quantification titled Analyzer for Neural Images by Matching Algorithm (ANIMA) was developed to search for and quantify GFAP signals from astrocyte cell bodies. The complete ANIMA algorithm can be found in the linked GitHub repository (https://github.com/thewindsofwinter/anima). The goal of this algorithm is to simulate the process by which a human would determine which pixels are parts of an astrocyte. In short, the ANIMA algorithm interprets an image of nuclei (a “guide”) as well as an image of astrocytes (the “analysis” image) as graphs. Then, the algorithm uses a simple breadth-first search to identify astrocytes which are in contact with one or more nuclei, calculates statistics for each cell body, and outputs all data in a cumulative CSV, as well as in individual text files and images. The following sections explain the ANIMA algorithm in detail.

A graphical user interface is used to allow users to upload the guide and analysis images. When the guide image is uploaded, the algorithm automatically identifies nuclei based on the fluorescence intensity of a nuclear marker DAPI (measured in the intensity of the blue component of the RGB value). The sum of the mean and standard deviation is used as a threshold for identifying cell edges. All pixels with a blue value above this heuristic are marked as part of a nucleus. In a similar

manner, when the analysis image is uploaded, the algorithm sets a threshold to identify astrocytes based on the intensity of GFAP fluorescence (white). The algorithm is designed with manual and automatic options. The manual option allows a user to set a threshold intensity between 0 and 255. The automatic option uses the mean and standard deviation of intensity within the analysis image to set an approximate threshold. After a threshold is set, all pixels with brightness higher than the threshold are marked as part of an astrocyte body.

Once the user uploads both images and pushes the "analyze" button, a simple breadth-first search is used to identify astrocytes which are in contact with nuclei. The algorithm iterates through all pixels until it finds some pixel not yet visited which is identified as a part of a nucleus as well as an astrocyte. The algorithm then marks the pixel as visited and performs the same operation on all unvisited pixels adjacent to the visited pixel which are marked as part of an astrocyte. In this manner, statistics such as the area, raw integrated density, overlap area, and mean intensity are calculated for each astrocyte which borders a nucleus.

After the image has been analyzed, all statistics are filtered. The current image analysis algorithm requires the astrocyte to be larger than 0.8 square micrometers and overlap at least 0.16 square micrometers with a neuron. These limits are provided to filter out small fragment astrocytes and astrocytes which are only marginally touching rather than engulfing a nucleus. The filtered statistics are then output in several formats. The statistics are appended to a cumulative CSV file. Additionally, a PNG image which shows the locations of all images is generated. This PNG image contains color-coded astrocytes in various shades of red, yellow, and green, with nuclei in purple. A text file is also generated containing the statistics and color for each astrocyte displayed in the PNG map. In this way, a user can determine which astrocyte candidates are truly engulfing one or more nuclei and perform a final manual filter on the data.

**14. Fluoro-Jade-C staining**

Coronal brain cryosections (20 µm thick) were subjected to Fluoro-Jade-C (FJ-C) staining using Ready-to-Dilute (RTD)™ Fluoro-Jade® C Staining Kit (Biosensis) with modifications. In brief, cryosections on slides were incubated for 5 min in Solution A containing Sodium Hydroxide (which were diluted 1:10 in 70% ethanol) in a Coplin jar. After washing in 70% ethanol and distilled water for 2 min each, the slides were incubated for 7 min in Solution B containing potassium permanganate (which were diluted 1:10 in distilled water) followed by 2 min rinsing in distilled water. Slides were then incubated for 7 min in part Solution C containing FJ-C and DAPI (which were diluted 1:10 in distilled water) in the dark. After 3 distilled water rinses for 1 min each, the slides were dried at 50-60°C for 5 min, cleared by immersion in xylene for 1-5 min, and then coverslipped with a non-aqueous, low fluorescent, styrene based mounting media, such as DPX. FJ-C-positive degenerating neurons were visualized with blue light excitation, while DAPI counter stained cell nuclei were visualized with ultra-violet illumination. To count the numbers of FJ-C-positive degenerating neurons per image, an intensity threshold was set to identify pixels that were FJ-C-positive within the image and manually counted in Image J.

**15. RNA isolation, reverse transcription, and real-time quantitative polymerase chain reaction (QPCR)**

Total RNA was extracted from the cells using the RNeasy Mini Kit (Qiagen) with on-column DNase treatment. Oligo-d$(T)_{23}$VN and random-primed cDNA was prepared from 2 µg of total RNA using the ProtoScript First Strand cDNA Synthesis Kit (New England Biolabs) and diluted 5-fold in water. One µL of diluted cDNA was used as template for QPCR analysis using a StepOnePlus Real-Time PCR System (Applied Biosystems) and validated primers. Primers were designed using Primer3 (https://primer3.org), and those that efficiently amplified single products of the expected size were used for QPCR. Primers included: Kcnq2 sense, 5'-CCCTGAAAGTCCAAGAGCAG-3'; Kcnq2 antisense, 5'-GTCGGTGCGTGAGAGGTTAG-3'; Gapdh sense, 5'-TGTTTCCTCGTCCCGTAGAC -3'; Gapdh antisense 5'-AATCTCCACTTTGCCACTGC-3'; Actb sense, 5'-AATCGTGCGTGACA TCAAAG-3'; Actb antisense 5'-CGTTGCCAATAGTGATGACC-3. QPCR was achieved using the following method: a denaturation and polymerase activation step at 95°C for 1 min and then 40

cycle consisting of 95°C for 10 s, 57°C for 10 s, and 72°C for 20 s. Data were analyzed using the comparative threshold cycle (Ct) method (22) and *Gapdh* control gene. Following normalization to Gapdh cDNA levels, which is reflected in the ΔCt values, the relative mRNA quantification (RQ) of the fold change for each condition compared to reference control was determined using the following equation: $RQ = 2^{(-\Delta Ct)} / 2^{(-\Delta Ct\ reference)}$. The RQ mean and standard error of the mean (SEM) are plotted.

**16. Statistical analysis**

All analyses are reported as mean ± SEM. The n values indicate number of mice. Origin Pro 9.5 (Origin Lab) was used to perform statistical analyses. Behavior data were analyzed using 2-way ANOVA with genotype as one factor and sex as the other. For imaging analyses, comparisons between two groups were conducted with the paired Student two-tailed *t* test, whereas Tukey tests and Fisher tests were used to establish post-hoc pair-wise differences between >2 groups. A priori value (P) < .05 was used to establish statistical significance.

## Supplemental Figures

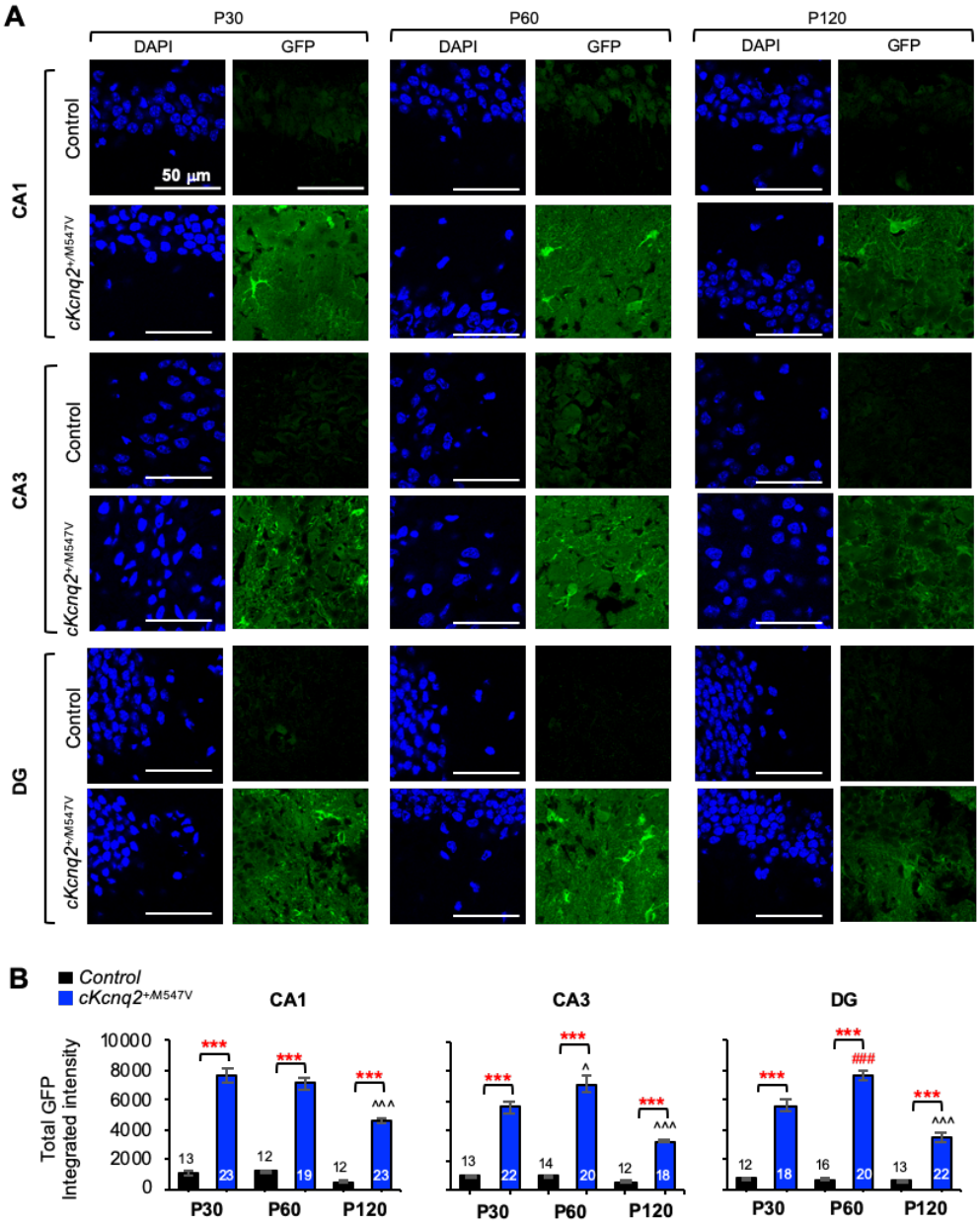


**Figure S1. Developmental expression of GFP in *cKcnq2*$^{+/M547V}$ mice.** Coronal brain cryosections of control mice (*Kcnq2*-M547V$^{fl/+}$) and *cKcnq2*$^{+/M547V}$ mice at P30, P60, and P120 were immunostained for EGFP, and counterstained with DAPI (nuclear marker). The confocal z-stack images (an optical section of 1.0 µm) were collected from hippocampal CA1, CA3, and dentate gyrus (DG) regions. **(A)** Representative fluorescence images of EGFP and DAPI in the hippocampi of the control and *cKcnq2*$^{+/M547V}$ mice. Scale bars: 50 µm. **(B)** Quantifications of background-subtracted GFP fluorescence intensity per image (size: 101.61 µm x 101.61 µm) of the hippocampi of the control and *cKcnq2*$^{+/M547V}$ mice. The numbers of images analyzed are indicated in the bar graphs. The number of mice used: n=1 female mouse per genotype at P30 and P60; n=2 female mice per genotype at P120. Data shown as mean ± SEM. Post-hoc Tukey test results are shown: ***$p < 0.005$ (control vs. *cKcnq2*$^{+/M547V}$); ^$p < 0.05$, ^^^$p < 0.005$ (P30 vs. P60 or P120 in *cKcnq2*$^{+/M547V}$ mice).

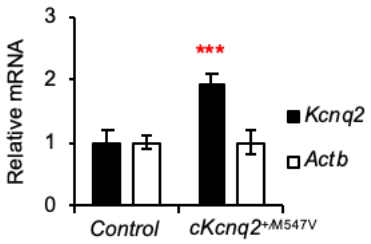


**Figure S2. Quantitative PCR analysis of $K_V7.2$ transcripts in control and *cKcnq2*$^{+/M547V}$ mice.** The cDNA was prepared from 2 μg of total RNA isolated from 2 hippocampi per mouse at P60 and used as template for QPCR analysis with the validated primers for *Kcnq2, Actb, and Gapdh*. Data were analyzed using the comparative threshold cycle (Ct) method and *Gapdh* control gene. Following normalization to *Gapdh* cDNA levels (which is reflected in the ΔCt values), the relative mRNA quantification (RQ) of the fold change for each condition compared to *Actb* reference gene was determined using the following equation: $RQ = 2^{(-\Delta Ct)} / 2^{(-\Delta Ct\ reference)}$. The RQ data shown as mean ± SEM. Two-tailed Student's T-test results are shown (***p<0.005). Sample sizes: Control (Emx1$^{cre/+}$): n=5 (2 males and 3 females). *cKcnq2*$^{+/M547V}$: n=5 (2 males and 3 females).

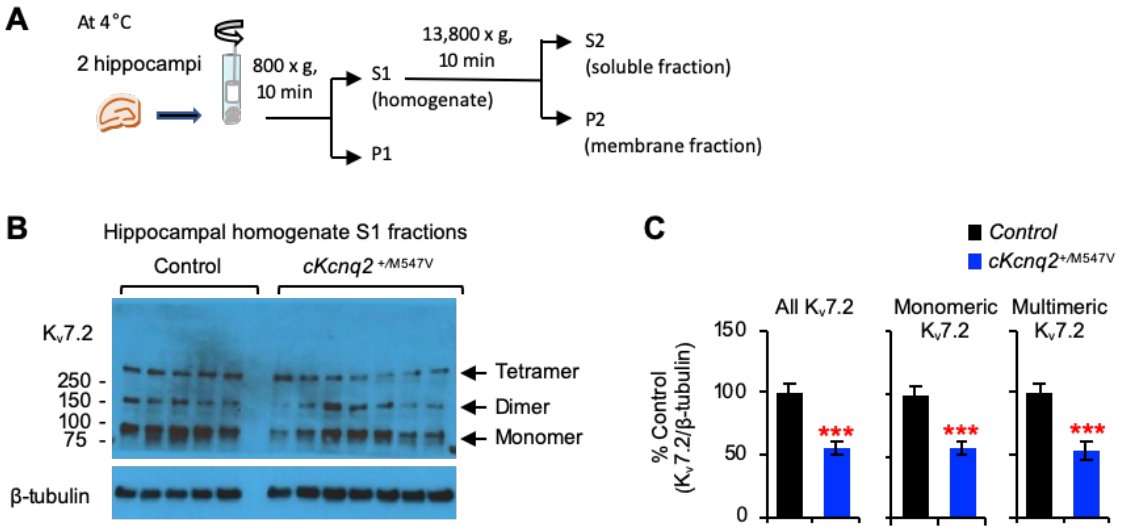


**Figure S3. $K_v$7.2 expression in control and *cKcnq2*$^{+/M547V}$ mice at P30. (A)** A schematic diagram of homogenization and fractionation of mouse hippocampal tissues. **(B)** Western blot images of $K_v$7.2 and β-tubulin in the hippocampal homogenates (S1) of *control* mice (*Kcnq2*-M547V$^{fl/+}$) and *cKcnq2*$^{+/M547V}$ mice at P30. **(C)** Quantification of all $K_v$7.2 bands (monomer, dimer, tetramer), $K_v$7.2 monomers, and $K_v$7.2 multimers (dimer, tetramer) in the hippocampal S1 fractions. The *cKcnq2*$^{+/M547V}$ mice displayed reduced hippocampal protein expression of $K_v$7.2 compared to control mice. Data shown as mean ± SEM. Two-tailed Student's t-test was performed. The total number of mice used for quantification at P30: *Control* mice (n=5) include 5 males. The *cKcnq2*$^{+/M547V}$ mice (n=7) include 5 males and 2 females.

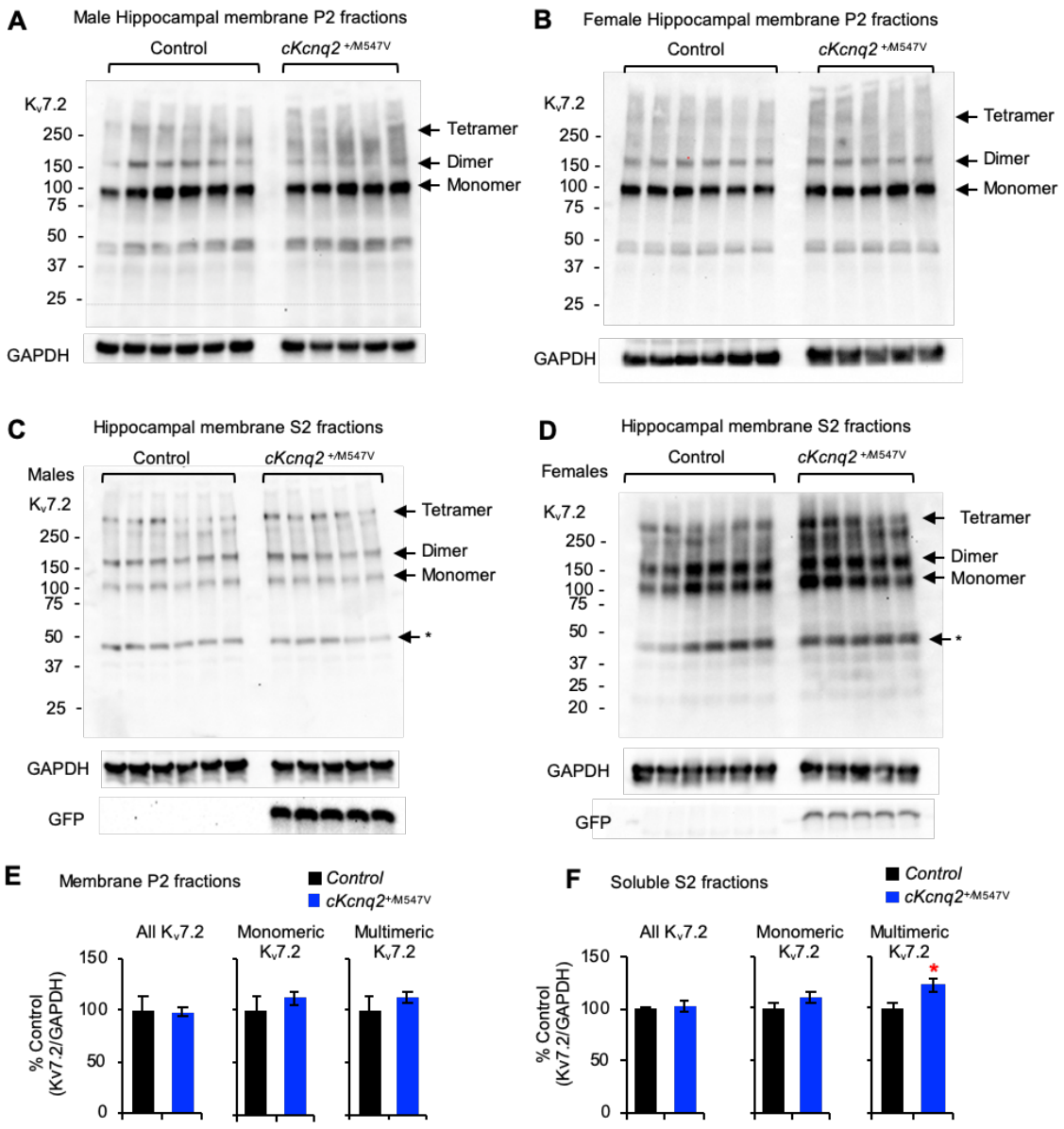


**Figure S4. $K_v7.2$ expression in control and *cKcnq2* $^{+/M547V}$ mice at P120.** Western blot images of $K_v7.2$ and GAPDH in the hippocampal membrane (P2) fractions (A, B, E) and soluble (S2) fractions (C, D, F) of control mice (Emx1$^{cre/+}$, *Kcnq2*-M547V$^{fl/+}$) and *cKcnq2*$^{+/M547V}$ mice at P120. Different exposure times were used for representative blots shown in A-D. **(A-B)** Representative western blot images of the hippocampal P2 fractions. **(C-D)** Representative western blot images of the hippocampal S2 fractions. **(E-F)** Quantification of all $K_v7.2$ bands (monomer, dimer, tetramer), $K_v7.2$ monomers, and $K_v7.2$ multimers (dimer, tetramer) in the hippocampal P2 fractions (E) and S2 fractions (F). The *cKcnq2*$^{+/M547V}$ mice displayed similar hippocampal protein expression of $K_v7.2$ compared to control mice. However, the expression of $K_v7.2$ multimers was increased in the hippocampal S2 fractions. Data shown as mean ± SEM. Two-tailed Student's T-test results are shown (*p<0.05). The total number of mice used for quantification at P120: *Control* mice (n=12) include 6 mice per sex (3 *Kcnq2*-M547V$^{fl/+}$and 3 Emx1$^{cre/+}$). The *cKcnq2*$^{+/M547V}$ mice (n=10) include 5 males and 5 females.

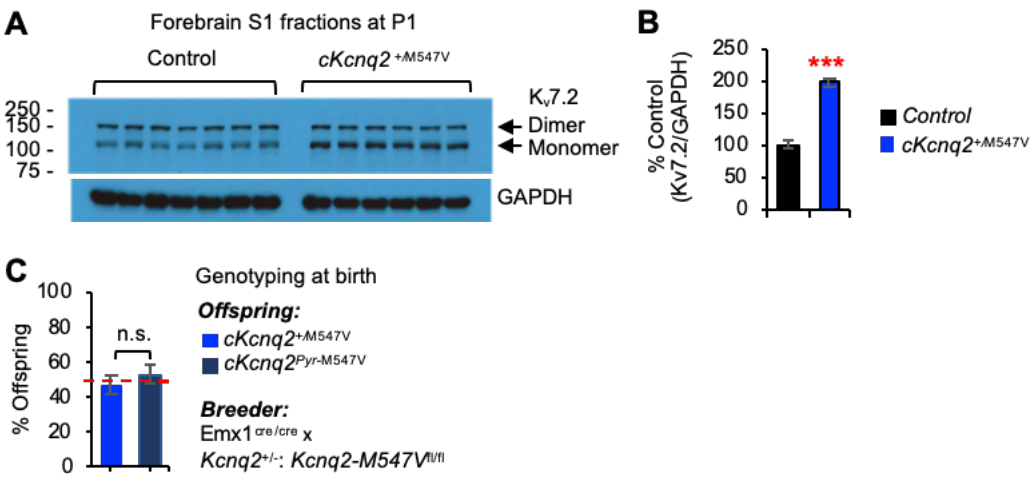


**Figure S5. $K_v$7.2 expression and Mendelian ratio in control and *cKcnq2*$^{+/M547V}$ mice at P1. (A)** Western blot images of $K_v$7.2 and GAPDH in the forebrain homogenates (S1) of *control* mice (*Kcnq2*$^{+/+}$) and *cKcnq2*$^{+/M547V}$ mice at P1. **(B)** Quantification of $K_v$7.2 in the S1 fractions. The *cKcnq2*$^{+/M547V}$ mice (n=6) displayed enhanced hippocampal protein expression of $K_v$7.2 compared to control mice (n=7). Two-tailed Student's t-test was performed (***$p < 0.005$). **(C)** Genotyping results at birth (n=38 collected from 4 breeding cages consisting of Emx1$^{cre/cre}$ x *Kcnq2*$^{+/-}$: *Kcnq2-M547V*$^{fl/fl}$) showed the expected Mendelian inheritance. Chi-square test was performed (n.s.: not significant). A dotted line indicates a 50% offspring mark. Data shown as mean ± SEM.

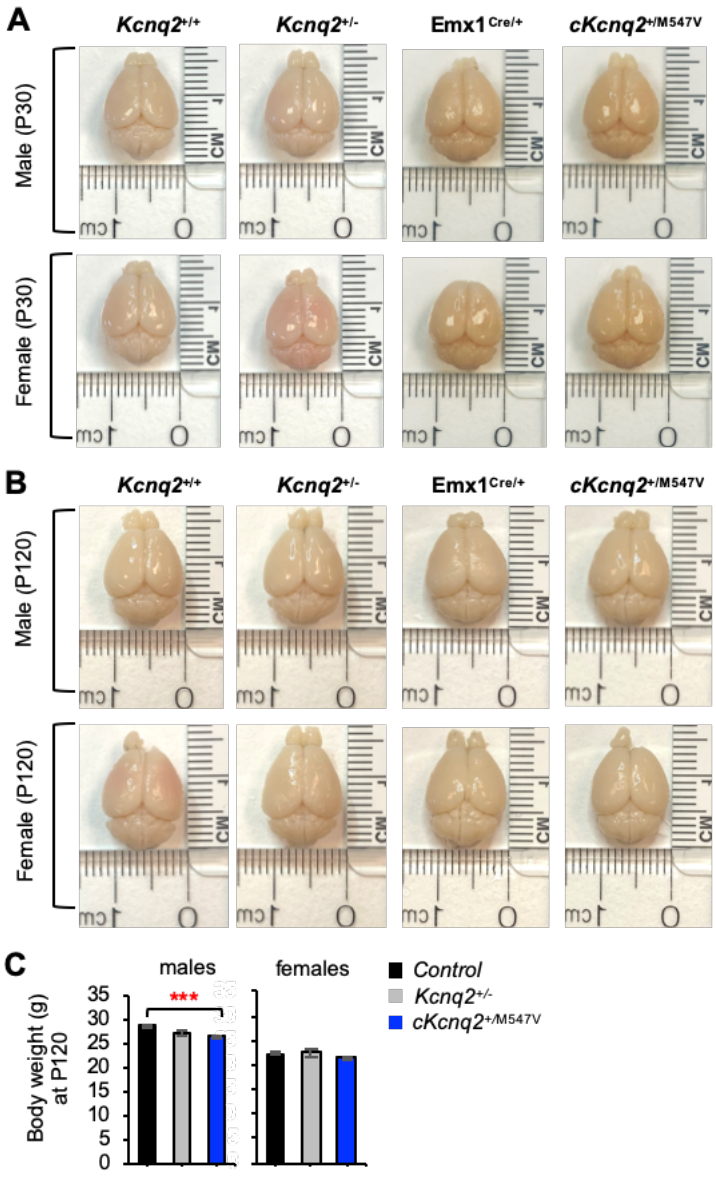


**Figure S6. The brain sizes and body weights of *control*, *Kcnq2* $^{+/-}$, and *cKcnq2*$^{+/M547V}$ mice.** **(A-B)** Conditional *cKcnq2*$^{+/M547V}$ mice displayed no obvious differences in the gross appearance and size of their brains compared to *Kcnq2*$^{+/-}$ and the control mouse brains. The control (*Kcnq2*$^{+/+}$, Emx1$^{cre/+}$), *Kcnq2*$^{+/-}$, and *cKcnq2*$^{+/M547V}$ mice at P30 and P120 were subjected to transcardial perfusion of 2% (w/v) paraformaldehyde, and their brains were dissected. **(A)** Photographs of brains collected at P30. **(B)** Photographs of brains collected at P120. **(C)** The body weights of *control*, *Kcnq2* $^{+/-}$, and *cKcnq2* $^{+/M547V}$ mice at P120. The total number of mice used: *Control* (male, n=27; female, n=30), *Kcnq2*$^{+/-}$ (male, n=10; female, n=12), *cKcnq2*$^{+/M547V}$ (male, n=15; female, n=19). Data shown as mean ± SEM. Post-hoc Tukey test results are shown (***$p < 0.005$).

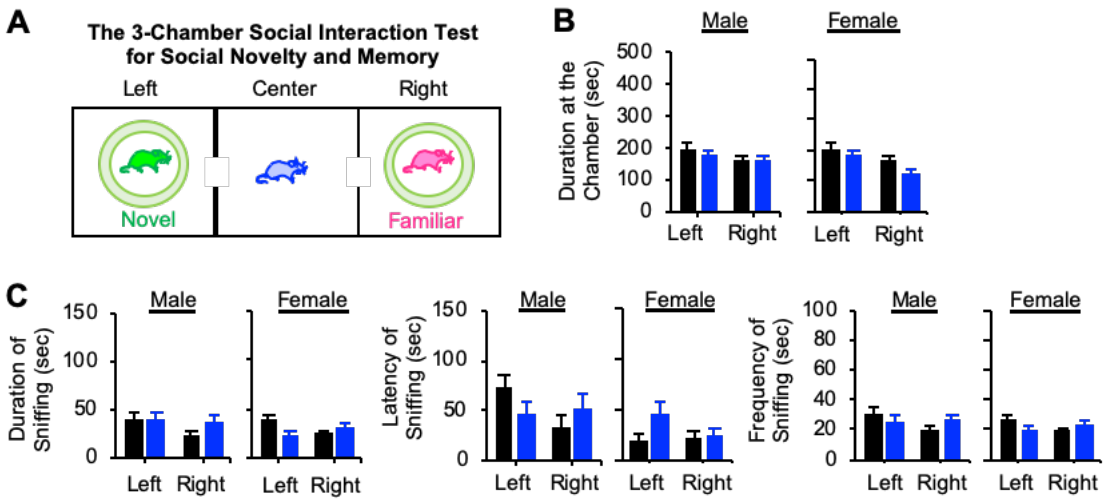


**Figure S7. Conditional *cKcnq2*$^{+/M547V}$ mice displayed normal social novelty preference.** After the completion of the 3-chamber social interaction test for "sociability" in Fig 3E, mice were subjected the "social novelty and memory" test. **(A)** In this test, a second novel stranger mouse-2 (another age-matched C57BL6) was placed inside the wire cage of the left chamber, and the test mouse (control or *cKcnq2*$^{+/M547V}$) was introduced into the center chamber and allowed to explore for 10 min. **(B)** Quantification of the time spent at left and right chambers. **(C)** Quantifications of the duration, latency, and frequency of sniffing behavior. The number of male mice used: Control *Kcnq2*-M547V$^{fl/+}$ (n=8), *cKcnq2*$^{+/M547V}$ (n=11). The number of female mice used: Control *Kcnq2*-M547V$^{fl/+}$ (n=8), *cKcnq2*$^{+/M547V}$ (n=11). Data shown as mean ± SEM. Post-hoc Tukey test results revealed no pair-wise difference among groups. Table S4 shows 2-way ANOVA test results per sex with chamber as one factor and genotype as the other.

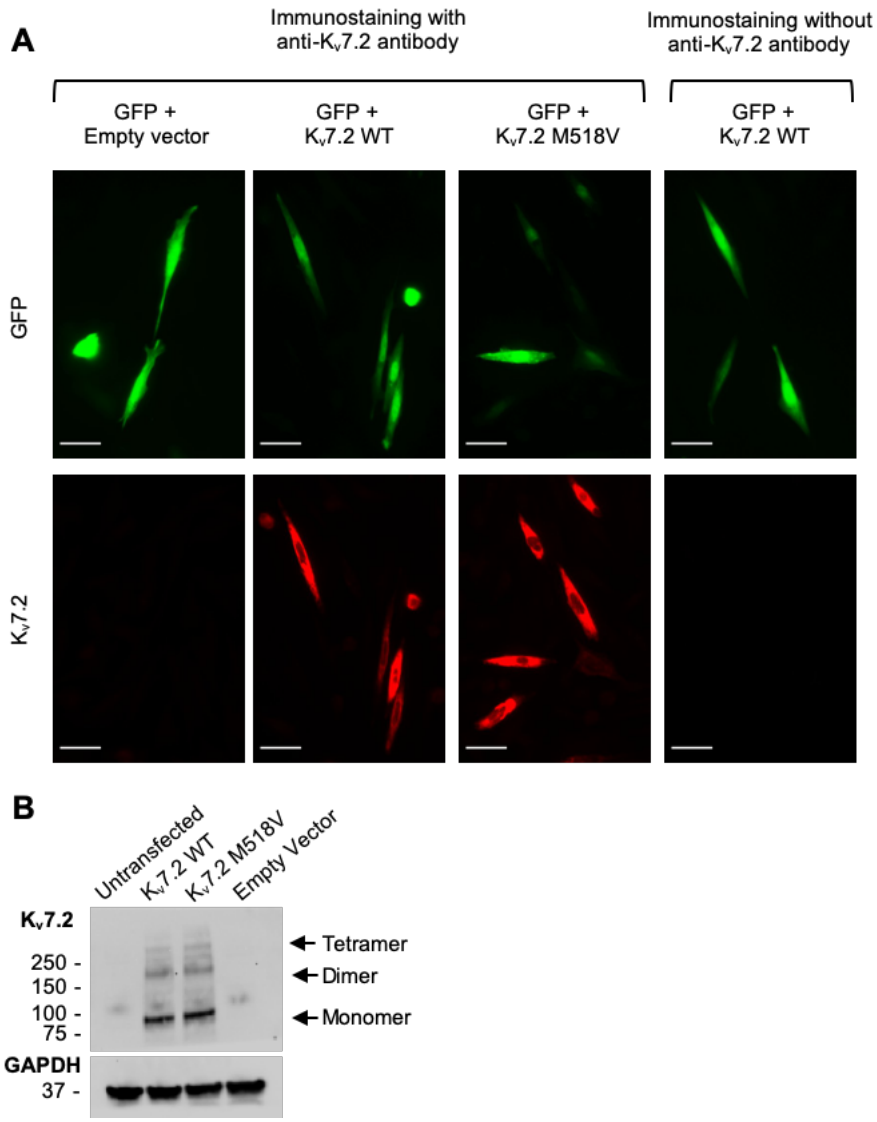


**Figure S8. The specificity of anti-$K_v$7.2 antibody used in Figure 4. (A)** Immunostaining of $K_v$7.2 in transfected CHO hm1 cells with anti-$K_v$7.2 antibody (Synaptic System). Cells were transfected with pEGFP-C1 (GFP) and pcDNA3 (Empty Vector), pcDNA3 containing the short isoform of human $K_v$7.2 (GenBank: Y15065.1, (21, 23)) wild-type (WT) or mutant containing EE mutation M518V which corresponds to M547V in murine $K_v$7.2 (GenBank: NM_010611.3). Anti-$K_v$7.2 antibody immunolabeled the cells transfected with $K_v$7.2 WT and $K_v$7.2-M518V, but not the cells transfected with GFP alone or when immunostaining was performed without primary antibody. Scale bars: 25 μm. **(B)** Western blot of lysates prepared from the CHO hm1 cells transfected with pcDNA3, pcDNA3-$K_v$7.2 WT, or pcDNA3-$K_v$7.2 M518V. Consistent with our previous report (19), immunoblotting with anti-$K_v$7.2 antibody (Synaptic System) revealed $K_v$7.2 as a monomer of ~90 kD and oligomers (a dimer of ~180 kD and a tetramer of ~360 kD) in cells transfected with $K_v$7.2 but not untransfected cells.

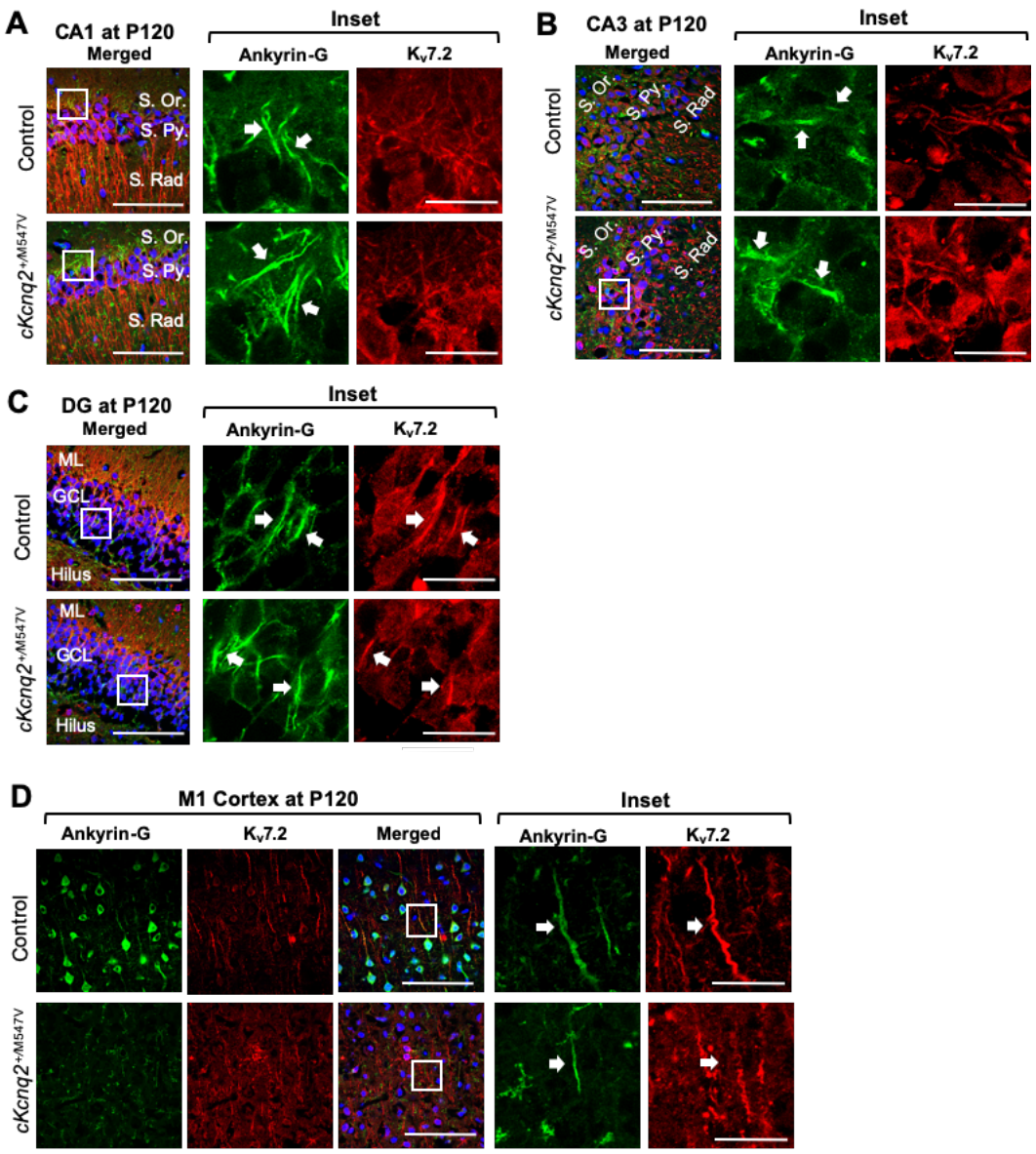


**Figure S9. $K_v7.2$ and Ankryin-G expression in the hippocampal and cortical pyramidal cells of *cKcnq2*$^{+/M547V}$ mice.** Coronal brain cryosections of *cKcnq2*$^{+/M547V}$ and control mice (*Kcnq2*-M547V$^{fl/+}$) at P120 were subjected to immunostaining for $K_v7.2$ and Ankyrin-G (AIS marker), and counterstained with DAPI (nuclear marker). **(A-C)** Merged representative images are identical to those in Figure 4A. $K_v7.2$ expression was observed in the Ankyrin-G-positive AIS in select DG pyramidal neurons but not in CA1 and CA3 neurons in both genotypes. Hippocampal pyramidal cell layers: *stratum pyramidale* (S. Py.), *stratum oriens* (S. Or.), and *stratum radiatum* (S. Rad.). Dentate Gyrus (DG) cell layers: granule cell layer (GCL), molecular layer (ML), and hilus. **(D)** The cortical pyramidal cells in control but not *cKcnq2*$^{+/M547V}$ mice displayed strong Ankyrin-G expression in the soma and AIS. The pial surface is at the top of each panel. Concentration of $K_v7.2$ at the AIS is seen in the control but not in *cKcnq2*$^{+/M547V}$ mice. Scale bars of the merged images in A-D: 100 μm. Scale bars in the Insets in A-D: 20 μm.

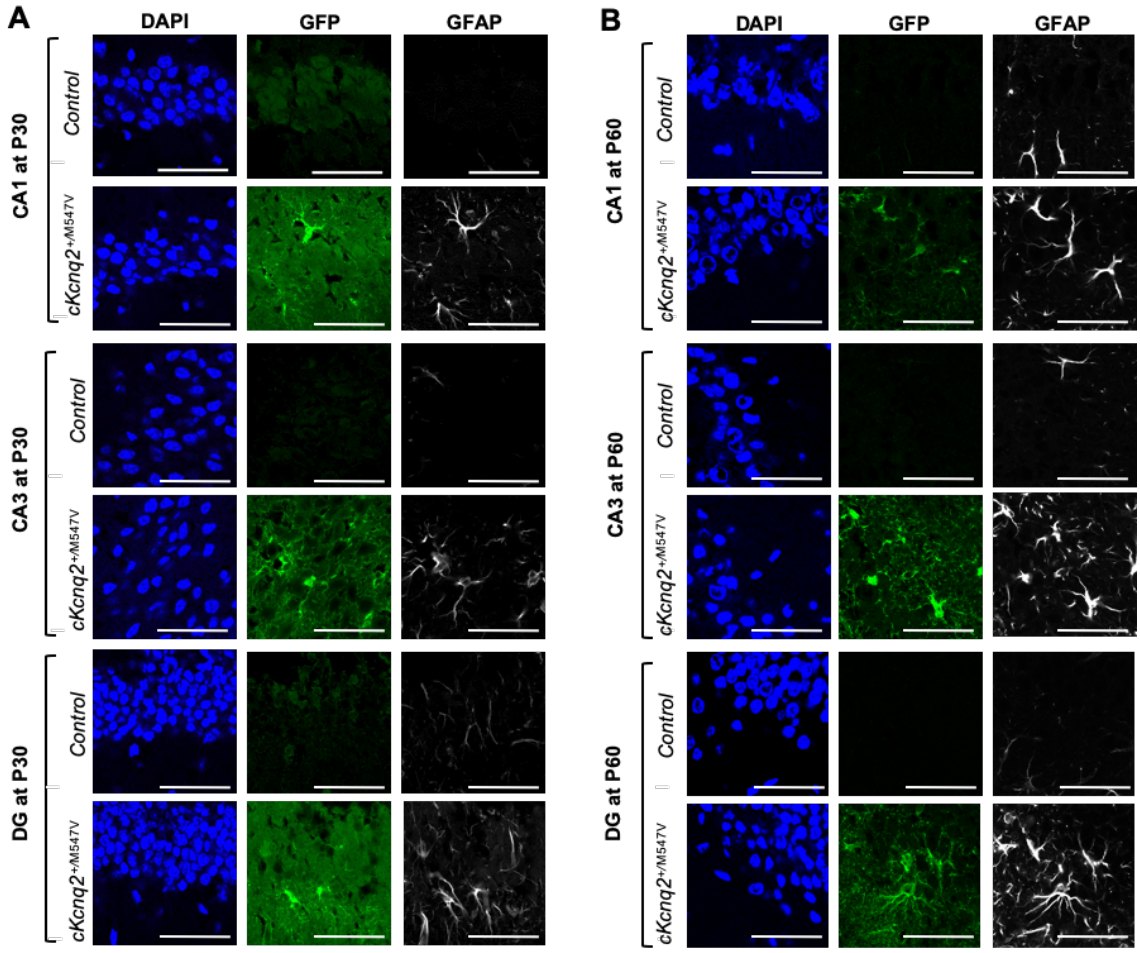


**Figure S10. Conditional *cKcnq2*$^{+/M547V}$ mice at P30 and P60 display reactive astrogliosis in the dorsal hippocampus. (A-B)** Coronal brain cryosections of *cKcnq2*$^{+/M547V}$ and control mice (*Kcnq2*-M547V$^{fl/+}$) at P30 (A) and P60 (B) were subjected to immunostaining for EGFP, and GFAP (astrocyte marker). Sections were counterstained with DAPI (nuclear marker). The confocal z-stack images (an optical section of 1.0 µm) were collected from hippocampal CA1, CA3, and dentate gyrus (DG) regions. Scale bars: 50 µm. Quantifications of the number of GFAP-positive cells within the image size (101.61 µm x 101.61 µm) and the mean background-subtracted GFAP fluorescence intensities (AU) per GFAP-positive cell in control and *cKcnq2*$^{+/M547V}$ mice are shown in Figure 4D-E.

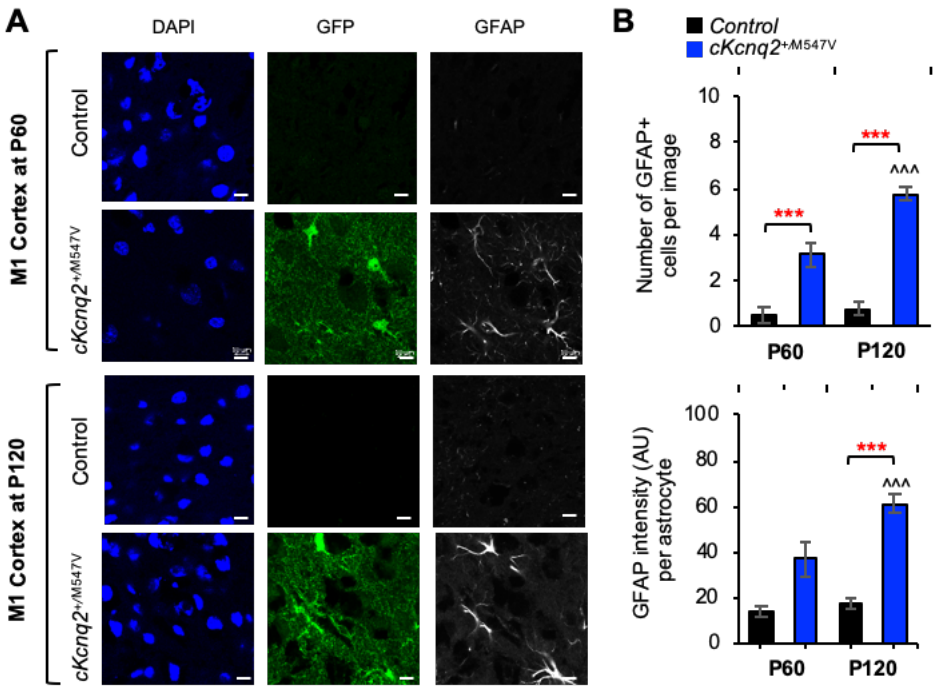


**Figure S11. Conditional *cKcnq2*$^{+/M547V}$ mice at P60 and P120 displayed increased number of reactive astrocytes in primary motor cortex.** Coronal brain cryosections of *cKcnq2*$^{+/M547V}$ and control mice (*Kcnq2*-M547V$^{fl/+}$) at P60 and P120 were subjected to immunostaining for EGFP and GFAP (astrocyte marker). Sections were counterstained with DAPI (nuclear marker). The confocal z-stack images (an optical section of 1.0 µm) were collected from the primary M1 motor cortex from the same sections that provided images in Fig. 4C. **(A)** Representative fluorescence images. Scale bars: 10 µm. **(B)** Quantifications of the number of GFAP-positive cells within the image size (101.61 µm x 101.61 µm) of the control mice (P60, n=6 images; P120, n=12 images) and *cKcnq2*$^{+/M547V}$ mice (P60, n=6 images; P120, n=14 images) and the mean background-subtracted GFAP fluorescence intensities (AU) per GFAP-positive cell in control mice (P60, n=6 cells in n=6 images; P120, n=18 cells in n=6 images) and *cKcnq2*$^{+/M547V}$ mice (P60, n=13 cells in n=7 images; P120, n=34 cells in n=10 images). Data shown as mean ± SEM. Post-hoc Tukey test results are shown: ***p < 0.005 (control vs. *cKcnq2*$^{+/M547V}$); ^^^p < 0.005 (P60 vs. P120 in *cKcnq2*$^{+/M547V}$ mice). The number of mice used: n=1 female mouse per genotype at P60; n=2 female mice per genotype at P120.

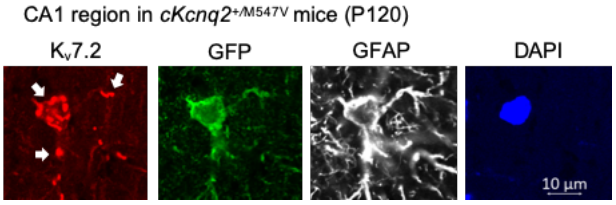


**Figure S12. GFP and $K_v$7.2 expression in hippocampal astrocytes of *cKcnq2*$^{+/M547V}$ mice.** Representative immunostained image of hippocampal CA1 region of a c*Kcnq2*$^{+/M547V}$ female mouse at P120 which show $K_v$7.2 proteins as large puncta and GFP expression in GFAP-positive astrocytes. DAPI is a nuclear marker. Scale bars: 10 µm.

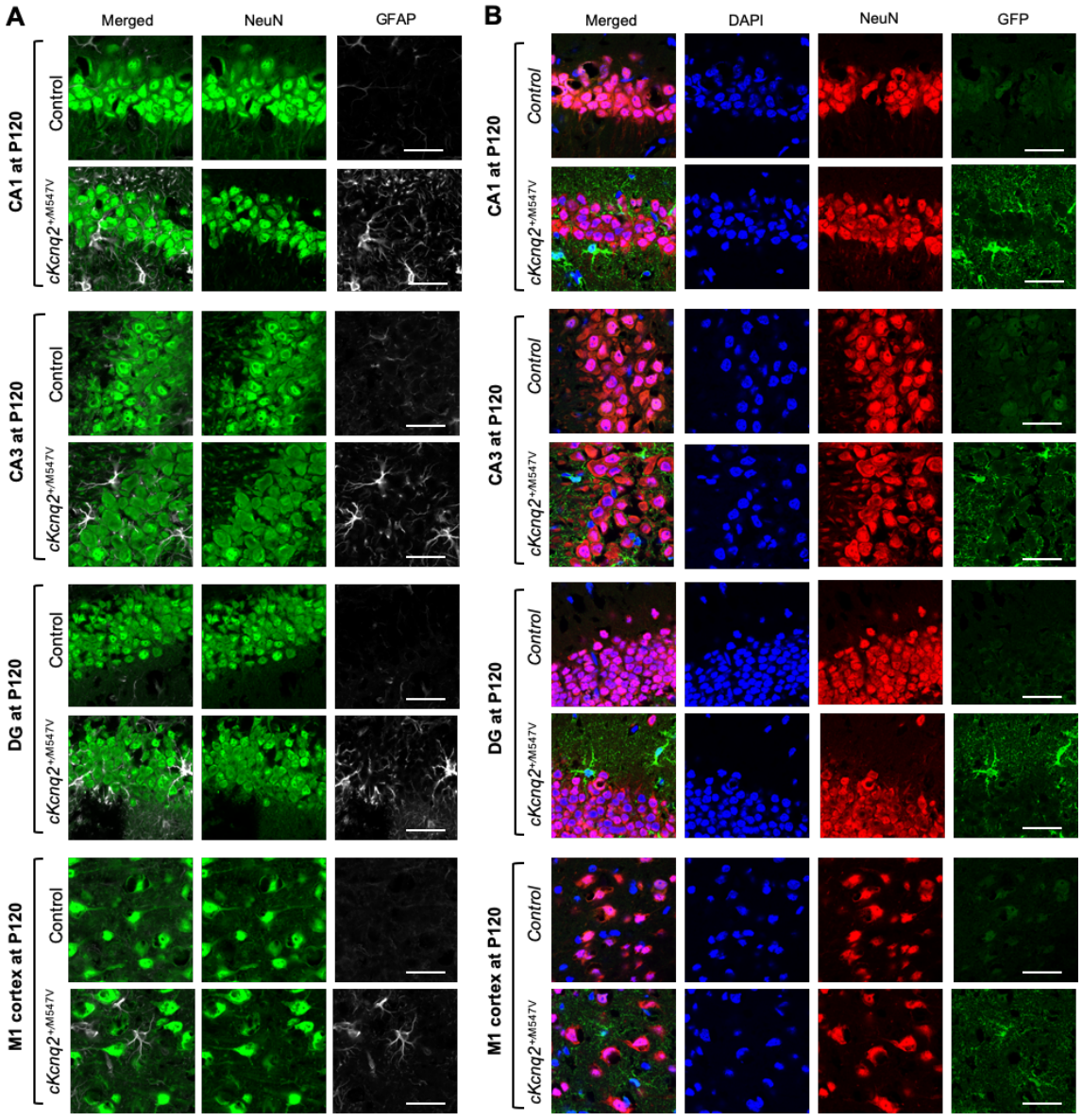


**Figure S13. Characterization of neurons and astrocytes in the control and *cKcnq2*$^{+/M547V/+}$ mice at P120. (A)** Coronal brain cryosections of *cKcnq2*$^{+/M547V}$ and control mice (*Kcnq2*-M547V$^{fl/+}$) at P120 were subjected to immunostaining for neuronal marker NeuN and astrocyte marker GFAP and visualized with secondary antibodies conjugated with Alexa488 and Alexa680, respectively. **(B)** Coronal brain cryosections of *cKcnq2*$^{+/M547V}$ and control mice (*Kcnq2*-M547V$^{fl/+}$) at P120 were subjected to immunostaining for NeuN and GFP and visualized with secondary antibodies conjugated with Alexa594 and Alexa488, respectively. The sections were counterstained with DAPI (nuclear marker). The confocal z-stack images (an optical section of 1.0 μm) were collected from hippocampal CA1, CA3, and dentate gyrus (DG) regions and the primary M1 motor cortex from the same sections. Scale bars: 50 μm.

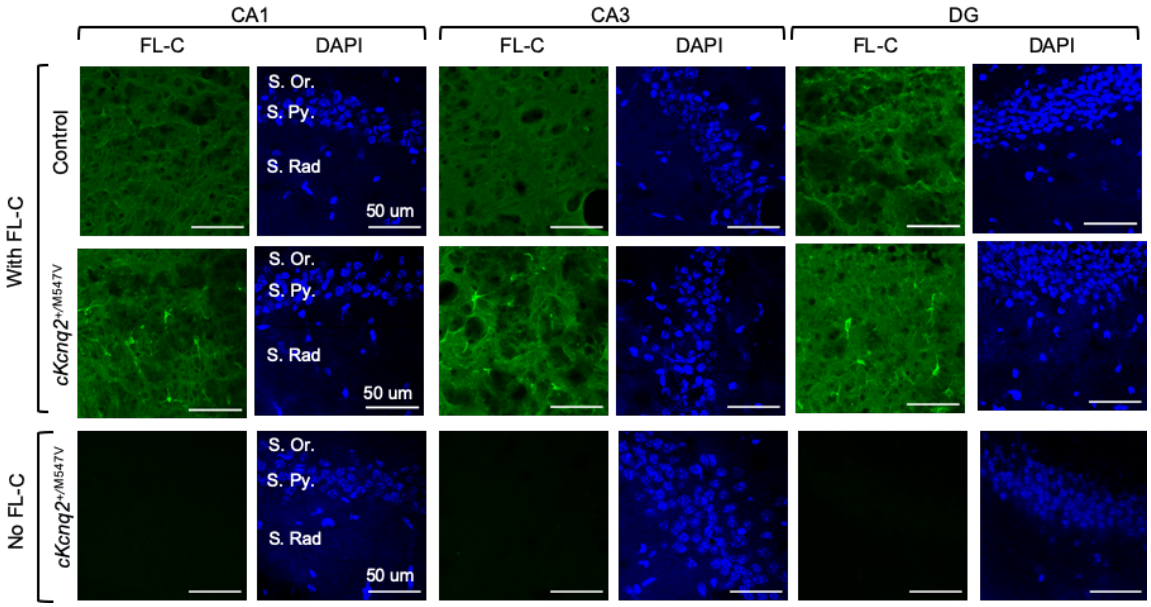


**Figure S14. Conditional *cKcnq2*$^{+/M547V}$ mice at P120 displayed increased number of degenerating neurons in the dorsal hippocampus. (A)** Coronal brain cryosections of *cKcnq2*$^{+/M547V}$ and control mice (*Kcnq2*-M547V$^{fl/+}$) at P120 were subjected to Fluoro-Jade C (FJ-C) and DAPI staining (with FL-C). Cryosections of *cKcnq2*$^{+/M547V}$ mouse brain were also subjected to the same staining procedure except the addition of Fluoro-Jade C stain as a negative control (No FL-C). The confocal z-stack images (an optical section of 1.0 μm) were collected from the dorsal hippocampi. Representative fluorescence images of FJ-C and DAPI in the hippocampi of the control and *cKcnq2*$^{+/M547V}$ mice at P120 are shown. Scale bars: 50 μm. **(B)** Quantifications of the numbers of FJ-C-positive degenerating neurons within the image size (160.04 μm x 160.04 μm) in the hippocampi of the control mice and *cKcnq2*$^{+/M547V}$ mice at P30, P60, and P120 are shown in Fig. 4B.

**Supplemental Tables**

**Table S1.** Two-way ANOVA statistical analysis for Figure 2D-G

| Behavior Test | Result | ANOVA table | F(DFn, DFd) | p value |
|---|---|---|---|---|
| Kainate-induced seizure | Cumulative seizure score | Sex | F(1, 43) = 3.10 | p = 0.086 |
| | | Genotype | F(2, 43) = 59.72 | p < 0.000 |
| | | Interaction | F(2, 43) = 1.40 | p = 0.257 |
| | Latency to stage 4 seizure (min) | Sex | F(1, 43) = 2.09 | p = 0.155 |
| | | Genotype | F(2, 43) = 61.11 | p < 0.000 |
| | | Interaction | F(2, 43) = 0.69 | p = 0.506 |
| | Latency to Death (min) | Sex | F(1, 43) = 0.05 | p = 0.832 |
| | | Genotype | F(2, 43) = 17.96 | p < 0.000 |
| | | Interaction | F(2, 43) = 0.60 | p = 0.552 |

**Table S2.** Two-way ANOVA statistical analysis for Figure 3A-D, F-G.

| Behavior Test | Result | ANOVA table | F(DFn, DFd) | p value |
|---|---|---|---|---|
| Rotarod | Latency to fall (sec) | Sex | F(1, 38) = 0.25 | p = 0.621 |
| | | Genotype | F(1, 38) = 1.62 | p = 0.211 |
| | | Interaction | F(1, 38) = 3.24 | p = 0.080 |
| Open field | Total distance in the arena (m) | Sex | F(1, 38) = 20.14 | p < 0.000 |
| | | Genotype | F(1, 38) = 6.98 | p = 0.012 |
| | | Interaction | F(1, 38) = 1.23 | p = 0.275 |
| | Number of entries into center | Sex | F(1, 38) = 2.55 | p = 0.119 |
| | | Genotype | F(1, 38) = 28.57 | p < 0.000 |
| | | Interaction | F(1, 38) = 0.04 | p = 0.835 |
| | Time in center (sec) | Sex | F(1, 38) = 0.30 | p = 0.585 |
| | | Genotype | F(1, 38) = 31.79 | p < 0.000 |
| | | Interaction | F(1, 38) = 0.55 | p = 0.463 |
| | Distance in center (m) | Sex | F(1, 38) = 2.87 | p = 0.098 |
| | | Genotype | F(1, 38) =25.80 | p < 0.000 |
| | | Interaction | F(1, 38) = 0.02 | p = 0.887 |
| Object Location test (OLT) | Discrimination index | Sex | F(1, 38) = 0.85 | p = 0.362 |
| | | Genotype | F(1, 38) = 8.87 | p = 0.005 |
| | | Interaction | F(1, 38) = 0.13 | p = 0.717 |
| | % total time of investigation | Sex | F(1, 38) = 0.85 | p = 0.362 |
| | | Genotype | F(1, 38) = 8.87 | p = 0.005 |
| | | Interaction | F(1, 38) = 0.13 | p = 0.717 |
| Novel Object recognition (NORT) | Discrimination index | Sex | F(1, 38) = 0.36 | p = 0.551 |
| | | Genotype | F(1, 38) = 9.31 | p = 0.004 |
| | | Interaction | F(1, 38) = 0.00 | p = 0.957 |
| | % total time of investigation | Sex | F(1, 38) = 0.36 | p = 0.551 |
| | | Genotype | F(1, 38) = 9.31 | p = 0.004 |
| | | Interaction | F(1, 38) = 0.00 | p = 0.957 |
| Grooming | Duration (sec) of grooming | Sex | F(1, 38) = 1.29 | p = 0.264 |
| | | Genotype | F(1, 38) = 14.14 | p = 0.001 |
| | | Interaction | F(1, 38) = 2.36 | p = 0.133 |
| | Latency (sec) of grooming | Sex | F(1, 38) = 6.35 | p = 0.016 |
| | | Genotype | F(1, 38) = 12.78 | p = 0.001 |
| | | Interaction | F(1, 38) = 0.35 | p = 0.556 |
| | Frequency of grooming | Sex | F(1, 38) = 0.00 | p = 0.971 |
| | | Genotype | F(1, 38) = 4.54 | p = 0.040 |
| | | Interaction | F(1, 38) = 0.76 | p = 0.390 |
| Marble Burying test | % of marbles buried | Sex | F(1, 38) = 1.29 | p = 0.264 |
| | | Genotype | F(1, 38) = 14.14 | p = 0.001 |
| | | Interaction | F(1, 38) = 2.36 | p = 0.133 |

**Table S3.** Two-way ANOVA statistical analysis for Figures 3E

| Behavior Test | Result | ANOVA table | F(DFn, DFd) | p value |
|---|---|---|---|---|
| Sociability | Duration at each chamber (sec) of males | Chamber | F(1, 34) = 120.3 | p < 0.0001 |
| | | Genotype | F(1, 34) = 0.47 | p = 0.498 |
| | | Interaction | F(1, 34) = 1.62 | p = 0.211 |
| | Duration at each chamber (sec) of females | Chamber | F(1, 40) = 30.87 | p < 0.0001 |
| | | Genotype | F(1, 40) = 0.00 | p = 0.155 |
| | | Interaction | F(1, 40) = 2.00 | p = 0.050 |
| | Duration of sniffing (sec) by males | Chamber | F(1, 34) = 58.38 | p < 0.001 |
| | | Genotype | F(1, 34) = 0.00 | p = 0.989 |
| | | Interaction | F(1, 34) = 0.28 | p = 0.597 |
| | Duration of sniffing (sec) by females | Chamber | F(1, 40) = 30.60 | p < 0.000 |
| | | Genotype | F(1, 40) = 5.71 | p = 0.022 |
| | | Interaction | F(1, 40) = 2.94 | p = 0.094 |
| | Latency of sniffing (sec) by males | Chamber | F(1, 34) = 26.53 | p < 0.000 |
| | | Genotype | F(1, 34) = 0.25 | p = 0.621 |
| | | Interaction | F(1, 34) = 1.21 | p = 0.279 |
| | Latency of sniffing (sec) by females | Chamber | F(1, 40) = 19.19 | p < 0.001 |
| | | Genotype | F(1, 40) = 0.03 | p = 0.855 |
| | | Interaction | F(1, 40) = 0.14 | p = 0.714 |
| | Frequency of sniffing by males | Chamber | F(1, 34) = 47.31 | p < 0.000 |
| | | Genotype | F(1, 34) = 0.33 | p = 0.570 |
| | | Interaction | F(1, 34) = 0.00 | p = 0.969 |
| | Frequency of sniffing by females | Chamber | F(1, 40) = 23.65 | p = 0.339 |
| | | Genotype | F(1, 40) = 5.88 | p = 0.020 |
| | | Interaction | F(1, 40) = 2.92 | p = 0.095 |

**Table S4.** Two-way ANOVA statistical analysis for Figure S3

| Behavior Test | Result | ANOVA table | F(DFn, DFd) | p value |
|---|---|---|---|---|
| Social Novelty | Duration at each chamber (sec) of males | Chamber | F(1, 34) = 4.90 | p = 0.034 |
| | | Genotype | F(1, 34) = 0.39 | p = 0.534 |
| | | Interaction | F(1, 34) = 0.37 | p = 0.546 |
| | Duration at each chamber (sec) of females | Chamber | F(1, 40) = 7.32 | p = 0.010 |
| | | Genotype | F(1, 40) = 2.79 | p = 0.103 |
| | | Interaction | F(1, 40) = 0.56 | p = 0.459 |
| | Duration of sniffing (sec) by males | Chamber | F(1, 34) = 3.50 | p = 0.070 |
| | | Genotype | F(1, 34) = 1.31 | p = 0.260 |
| | | Interaction | F(1, 34) = 1.27 | p = 0.267 |
| | Duration of sniffing (sec) by females | Chamber | F(1, 40) = 0.54 | p = 0.468 |
| | | Genotype | F(1, 40) = 0.74 | p = 0.394 |
| | | Interaction | F(1, 40) = 6.64 | p = 0.014 |
| | Latency of sniffing (sec) by males | Chamber | F(1, 34) = 2.62 | p = 0.114 |
| | | Genotype | F(1, 34) = 0.00 | p = 0.977 |
| | | Interaction | F(1, 34) = 3.96 | p = 0.055 |
| | Latency of sniffing (sec) by females | Chamber | F(1, 40) = 1.04 | p = 0.315 |
| | | Genotype | F(1, 40) = 3.07 | p = 0.087 |
| | | Interaction | F(1, 40) = 1.76 | p = 0.192 |
| | Frequency of sniffing by males | Chamber | F(1, 34) = 1.88 | p = 0.179 |
| | | Genotype | F(1, 34) = 0.00 | p = 0.964 |
| | | Interaction | F(1, 34) = 2.66 | p = 0.112 |
| | Frequency of sniffing by females | Chamber | F(1, 40) = 0.62 | p = 0.436 |
| | | Genotype | F(1, 40) = 0.62 | p = 0.436 |
| | | Interaction | F(1, 40) = 7.03 | p = 0.011 |

**Supplemental Videos**

**Movie S1:** An example of a male *cKcnq2*$^{+/M547V}$ mouse displaying an abnormal behavior in their home cage such as continuous jumping.
**File name and format:** Video-S1_jumping.mov

**Movie S2**: An example of a male *cKcnq2*$^{+/M547V}$ mouse displaying an abnormal behavior in their home cage such as continuous digging.
**File name and format:** Video-S2_digging.mov

**Movie S3:** An example of a male *cKcnq2*$^{+/M547V}$ mouse which appeared to be in sleep due to their motionless and inert postures with their eyes closed.
**File name and format:** Video-S3_motionless.mov

**Movie S4:** A female *cKcnq2*$^{+/M547V}$ mouse in Fig. 2B which displayed stage 7 seizures during video-EEG recording.
**File name and format:** Video-S4_Stage7-Seizure-EEG_Fig2B-Female.mov

**Movie S5:** A female *cKcnq2*$^{+/M547V}$ mouse in Fig. 2C which displayed stage 7 seizures during video-EEG recording.
**File name and format:** Video-S5_Stage4-Seizure-EEG_Fig2C-Female.mov

**SI References**


1. S. Erwood, B. Gu, Embryo-Based Large Fragment Knock-in in Mammals: Why, How and What's Next. *Genes (Basel)* **11** (2020).
2. B. Hall *et al.*, Genome Editing in Mice Using CRISPR/Cas9 Technology. *Curr Protoc Cell Biol* **81**, e57 (2018).
3. A. V. Tzingounis, R. A. Nicoll, Contribution of KCNQ2 and KCNQ3 to the medium and slow afterhyperpolarization currents. *Proc Natl Acad Sci U S A* **105**, 19974-19979 (2008).
4. E. C. Kim *et al.*, Heterozygous loss of epilepsy gene KCNQ2 alters social, repetitive and exploratory behaviors. *Genes Brain Behav* **19**, e12599 (2020).
5. J. Clasadonte, J. Dong, D. J. Hines, P. G. Haydon, Astrocyte control of synaptic NMDA receptors contributes to the progressive development of temporal lobe epilepsy. *Proc Natl Acad Sci U S A* **110**, 17540-17545 (2013).
6. C. A. Christian *et al.*, Endogenous positive allosteric modulation of GABA(A) receptors by diazepam binding inhibitor. *Neuron* **78**, 1063-1074 (2013).
7. M. L. Casalia, M. A. Howard, S. C. Baraban, Persistent seizure control in epileptic mice transplanted with gamma-aminobutyric acid progenitors. *Ann Neurol* **82**, 530-542 (2017).
8. J. P. Pinel, L. I. Rovner, Electrode placement and kindling-induced experimental epilepsy. *Exp Neurol* **58**, 335-346 (1978).
9. R. Paylor, C. M. Spencer, L. A. Yuva-Paylor, S. Pieke-Dahl, The use of behavioral test batteries, II: effect of test interval. *Physiol Behav* **87**, 95-102 (2006).
10. K. L. McIlwain, M. Y. Merriweather, L. A. Yuva-Paylor, R. Paylor, The use of behavioral test batteries: effects of training history. *Physiol Behav* **73**, 705-717 (2001).
11. J. K. Denninger, B. M. Smith, E. D. Kirby, Novel Object Recognition and Object Location Behavioral Testing in Mice on a Budget. *J Vis Exp* 10.3791/58593 (2018).
12. A. V. Kalueff *et al.*, Neurobiology of rodent self-grooming and its value for translational neuroscience. *Nat Rev Neurosci* **17**, 45-59 (2016).
13. M. Angoa-Perez, M. J. Kane, D. I. Briggs, D. M. Francescutti, D. M. Kuhn, Marble burying and nestlet shredding as tests of repetitive, compulsive-like behaviors in mice. *J Vis Exp* 10.3791/50978, 50978 (2013).
14. J. A. Zombeck, E. K. Deyoung, W. J. Brzezinska, J. S. Rhodes, Selective breeding for increased home cage physical activity in collaborative cross and Hsd:ICR mice. *Behav Genet* **41**, 571-582 (2011).
15. P. J. Clark *et al.*, Intact neurogenesis is required for benefits of exercise on spatial memory but not motor performance or contextual fear conditioning in C57BL/6J mice. *Neuroscience* **155**, 1048-1058 (2008).
16. S. S. Moy *et al.*, Sociability and preference for social novelty in five inbred strains: an approach to assess autistic-like behavior in mice. *Genes Brain Behav* **3**, 287-302 (2004).
17. M. Yang, J. L. Silverman, J. N. Crawley, Automated three-chambered social approach task for mice. *Curr Protoc Neurosci* **Chapter 8**, Unit 8 26 (2011).
18. B. C. Baculis *et al.*, Prolonged seizure activity causes caspase dependent cleavage and dysfunction of G-protein activated inwardly rectifying potassium channels. *Sci Rep* **7**, 12313 (2017).
19. J. Zhang *et al.*, Identifying mutation hotspots reveals pathogenetic mechanisms of KCNQ2 epileptic encephalopathy. *Sci Rep* **10**, 4756 (2020).
20. H. J. Chung, Y. N. Jan, L. Y. Jan, Polarized axonal surface expression of neuronal KCNQ channels is mediated by multiple signals in the KCNQ2 and KCNQ3 C-terminal domains. *Proc Natl Acad Sci U S A* **103**, 8870-8875 (2006).
21. E. C. Kim *et al.*, Reduced axonal surface expression and phosphoinositide sensitivity in Kv7 channels disrupts their function to inhibit neuronal excitability in Kcnq2 epileptic encephalopathy. *Neurobiol Dis* **118**, 76-93 (2018).
22. T. D. Schmittgen, K. J. Livak, Analyzing real-time PCR data by the comparative C(T) method. *Nat Protoc* **3**, 1101-1108 (2008).
23. G. Orhan *et al.*, Dominant-negative effects of KCNQ2 mutations are associated with epileptic encephalopathy. *Ann Neurol* **75**, 382-394 (2014).